XIII International Conference on Computational Plasticity. Fundamentals and Applications
COMPLAS XIII
E. Oñate, D.R.J. Owen, D. Peric and M. Chiumenti (Eds)

# ADVANCED MATERIAL MODEL FOR SHEAR CUTTING OF METAL SHEETS

**FLORIAN GUTKNECHT*, FRANK STEINBACH*, TILL CLAUSMEYER* AND A. ERMAN TEKKAYA***

* Institute of Forming Technology and Lightweight Construction (IUL)
Department of Mechanical Engineering, Technische Universität Dortmund
Baroper Str. 303, 44227 Dortmund, Germany
e-mail: Florian.Gutknecht@iul.tu-dortmund.de, www.iul.eu

**Keywords:** sheet metal, blanking, cutting surface, damage model, simulation.

**Abstract.** A finite-element simulation of the shear cutting process is used to predict the geometry of the cutting surface. A fully-coupled Lemaitre-type model is used in the process model for the description of the material behaviour. The extended Lemaitre model considers the influence of shear and compression-dominated stress states on the propagation of damage. Tensile tests with and without notches are used for the identification of material parameters. These methods are advantageous for the analysis of different blanking processes.
Since damage parameters have a strong influence on the cutting surface quality, a numerical study is conducted to analyse their influence. The results of the simulations are compared with experimental data.

## 1 INTRODUCTION

The knowledge of the underlying physics of blanking operations yields valuable information for users of this technology. As single or multiple blanking operations occur in the process chain of virtually all sheet metal parts, a physical analysis of the blanking process has high technological relevance. In particular, the knowledge of the stress state is important because it provides information on the load of tools, but is also closely connected to the attributes of the finished product, such as the cut surface quality. The properties of the cutting surface are determined by the fracture behaviour as the material is separated. The fracture behaviour itself depends on the stress state.
Goijaerts et al. [1] proposed a complex and a simple identification strategy for uncoupled damage criteria and evaluated them in blanking simulations. It was found that the maximum force could be predicted quite well, if the complex identification was chosen. However the setup was not suitable to gain in-depth understanding of the process, as uncoupled models cannot represent the softening behaviour of ductile steels. Hambli et al. [2, 3] concluded that the original Gurson and Lemaitre model as typical coupled damage models lack satisfying results, due to their missing capabilities to consider low triaxiality. Dalloz et al. [4] on the other hand showed good agreement of the simulation with experiments, for Gurson's model

using a different parameter set. Due to these results it was decided to investigate Lemaitre's damage model with an enhancement for low triaxiality. Although several researchers have investigated this challenging topic, there is still no standard way to solve this task.
The next chapter will start with a brief summary of the necessary continuum mechanical framework and afterwards present the employed constitutive law. Chapter 3 is dedicated to the process of parameter identification. It will show the strategy and list the setups for experiments and simulations. In chapter 4 results of parameter identification and shear cutting simulation will be presented and discussed. This paper will end with conclusion in chapter 5.

## 2 MATERIAL MODEL

An essential aspect of the FE-model for the simulation of blanking is the material model. It has to consider the work-hardening during plastic deformation as well as the softening prior to rupture. In the present paper an elastic-plastic Lemaitre-type damage model [5, 6] is applied. The formulation is reviewed in the following.

### 2.1 Kinematics

The deformation gradient $\mathbf{F}$ transforms line elements in the reference configuration into line elements in the current configuration. The kinematic framework of the current model relies on the material stretch tensor $\mathbf{U} := \sqrt{\mathbf{C}}$ in terms of the right Cauchy-Green tensor $\mathbf{C} := \mathbf{F}^{\mathrm{T}} \bullet \mathbf{F}$. For metal forming applications it is useful to work with the logarithmic material strain tensor

$$\mathbf{E} := \ln(\mathbf{U}) \tag{1}$$

A work-conjugate stress measure $\mathbf{T}$ to the logarithmic strain $\mathbf{E}$ is obtained through

$$\partial_t w = \mathbf{P} : \partial_t \mathbf{F} = \mathbf{T} : \partial_t \mathbf{E} \tag{2}$$

in terms of the stress where $\mathbf{P}$ is the first Piola-Kirchhoff or nominal stress tensor. The kinematic framework follows [6]. An additive decomposition of the logarithmic strain

$$\mathbf{E} = \mathbf{E}^e + \mathbf{E}^p \tag{3}$$

into elastic and plastic parts $\mathbf{E}^e$ and $\mathbf{E}^p$, respectively is assumed.

### 2.2 Constitutive behaviour

The effect of ductile damage is considered by the internal damage variable $D \in [0,1]$. It accounts for the decrease of the load bearing capacity due to the occurrence of defects. The effective stress $\tilde{\mathbf{T}} = \mathbf{T} / (1 - D)$ represents the stress acting on the undamaged area, as opposed to the stress $\mathbf{T}$ acting on the total area. The Helmholtz free energy

$$\Psi(\mathbf{E}^e, \alpha, D) = \Psi^e(\mathbf{E}^e, D) + \Psi^p(\alpha) \tag{4}$$

is additively decomposed into elastic and plastic parts $\Psi^e$ and $\Psi^p$, respectively. $\alpha$ represents the equivalent plastic strain. Within the framework of thermodynamics one obtains

$$\left.\begin{aligned} \mathbf{T} &= \partial_{\mathbf{E}^e}\Psi(\mathbf{E}^e,\,\alpha, D),\\ q &= \partial_{\alpha}\Psi(\mathbf{E}^e,\alpha, D),\\ Y &= \partial_{D}\Psi(\mathbf{E}^e,\alpha, D) \end{aligned}\right\}. \tag{5}$$

for the stress $\mathbf{T}$, the isotropic hardening $q$, and the driving force for the evolution of damage $Y$. For isotropic plastic behaviour the dissipation potential reads $\Phi = \Phi^p(\tilde{\mathbf{T}},\, q, D) + \Phi^d(Y, D).$ The evolution relations for the plastic strain rate tensor, the equivalent plastic strain and the damage variable are obtained as

$$\left.\begin{aligned} \dot{\mathbf{E}}^p &= \lambda\partial_{\mathbf{T}}\Phi(\tilde{\mathbf{T}}, q, Y, D),\\ \dot{\alpha} &= \lambda\partial_{q}\Phi(\tilde{\mathbf{T}}, q, Y, D),\\ \dot{D} &= \lambda\,\partial_{Y}\Phi(\tilde{\mathbf{T}}, q, Y, D). \end{aligned}\right\}. \tag{6}$$

in the framework of associated plasticity. $\lambda$ denotes the plastic multiplier. For rate-independent plasticity the consistency condition $\lambda\Phi = 0$ has to be fulfilled. In the current paper we work with the special forms

$$\begin{aligned} \Psi^e(\mathbf{E}^e, D) &= (1-D)\left(\frac{1}{2}\lambda_1\left(\operatorname{tr}\left(\mathbf{E}^e\right)\right)^2 + \mu\,\operatorname{tr}\left(\left(\mathbf{E}^e\right)^2\right)\right),\\ \Psi^p(\alpha) &= \frac{C}{n+1}(\alpha-\varepsilon_0)^{n+1} \end{aligned} \tag{7}$$

where $C$, $\varepsilon_0$ and $n$ represent material parameters governing isotropic Swift hardening. The plastic potential is given by $\Phi^p(\mathbf{T}, q, D) = \tilde{\sigma}_{eq} - q = \sqrt{3/2\;\operatorname{dev}(\tilde{\mathbf{T}}):\operatorname{dev}(\tilde{\mathbf{T}})} - q$. The damage potential

$$\Phi^d = \frac{S}{(\kappa+1)}\left\langle\frac{Y-Y_0}{S}\right\rangle^{\kappa+1}\frac{1}{(1-D)^{\beta}} \tag{8}$$

depends on the driving force $Y := Y^+$ and the material parameters $S$, $\beta$, $\kappa$. $\langle x\rangle = (|x| + x)/2$ represents the MacCauley bracket. In the context of blanking simulations it is important to consider that the evolution of damage is retarded for compressive stress states. Therefore, the weighting factor $h$ is introduced

$$Y^+ = \frac{1+\nu}{2E}\left\{\sum_{i=1}^{3}\left[\left\langle\tilde{T}_i\right\rangle^2 + h\left\langle-\tilde{T}_i\right\rangle^2\right]\right\} - \frac{9\nu}{2E}\left\{\sum_{i=1}^{3}\left[\left\langle\tilde{p}\right\rangle^2 + h\left\langle-\tilde{p}\right\rangle^2\right]\right\} \tag{9}$$

to consider the effect of compressive stress states on the driving force. Here, $\tilde{T}_i$ represent the principle stresses of $\tilde{\mathbf{T}}$ and $\tilde{p} := 1/3\;\operatorname{tr}(\tilde{T})$ the hydrostatic pressure. Combining (7) and (9), the particular form of the damage evolution is

$$\dot{D} = \left\langle\frac{Y-Y_0}{S}\right\rangle^{\kappa}\frac{1}{(1-D)^{\beta}} \tag{10}$$

The model is implemented via the user material interface into Abaqus Explicit. Details of the model formulation and the implementation are given in [6]. The standard damage model of

Lemaitre [7] does not distinguish between compressive stresses and tensile stresses for the evolution of damage. With the original Lemaitre model [7], i.e. $h = 1$ in (9), one obtains a fracture curve which does not consider the sign of triaxiality. This is in contrast to experimental observations, e.g. of Bao et al. [8]. In general, for technical metals, fracture occurs at higher strains for compressive stresses. Thus the fracture strain for triaxiality = - 1/3 tends asymptotically to infinity in the current model for the limiting case of $h = 0$.

## 3 PARAMETER IDENTIFICATION

Since the aim of the current paper is to investigate manufacturing processes such as blanking with the help of the presented model, material parameters need to be identified on the basis of suitable experiments. As discussed in the introduction, previous researchers have proposed a number of strategies involving different experiments and identification strategies. In the current work a strategy is chosen, which takes the important features of the material model, the geometry of the as-received material and the targeted forming process into account. In the following relevant aspects of the tested material are described. Details of experiments used for characterization are presented. With this information at hand, the strategy to determine the material parameters governing the elastic-plastic behaviour ($E$, $\upsilon$, $C$, $\varepsilon_0$, $n$) and the damage behaviour ($Y_0$, $\beta$, $\kappa$, $S$, $D_c$) is outlined. Here, $D_c$ represents a parameter, which determines the critical value of the damage variable $D$. For values of $D$ greater than $D_c$, it is assumed that the load-bearing capacity of the material is reached. The identification strategy involves an analytical consideration of the effect of single parameters on the physical behaviour and a numerical optimization strategy. The identified material parameters can then be used for the process simulation of blanking, which is shortly described.

### 3.1 Investigated Material

The following experimental tests are performed with the dual-phase steel DP600 from ThyssenKrupp Steel Europe. The sheets are delivered as single sheets with dimensions 1000 mm x 50 mm x 1 mm. The elastic constants are determined as: Young's modulus $E$ = 201 GPa, Poisson ratio is assumed as $\upsilon=0.3$. The initial yield stress $\sigma_Y$ is which governs the onset of plastic yielding is determined as 386 MPa.

### 3.2 Experiments for material characterization

A suitable selection of characterization experiments has to generate data which allows the observation of the behaviour in the elastic-plastic regime and for larger deformation the occurrence of softening, which might be followed by fracture. Uniaxial tension tests are performed for the characterization of the elastic-plastic behaviour, while tensile tests with a notched specimen geometry are selected for the analysis of damage and fracture behaviour.
All tensile tests are performed with the universal testing machine (Zwick Z250) and only in rolling direction, due to the restricted dimensions of the delivered material. The cross-head velocity is set to 0.2 mm/s, resulting in a nominal strain-rate of 0.0025 1/s for the uniaxial tension tests. The geometry of the specimens for the uniaxial tensile test is chosen according to DIN 50125.
For the identification of the material parameters in the post-necking regime a slightly different setup is chosen. Instead of standardized tensile specimen, notched tensile specimen are used.

The specimen has a gauge length of 15 mm, width of 10 mm and unchanged thickness of 1 mm. Within the gauge area are two notches symmetric to the longitudinal axis with a radius of 2.5 mm. The cross-head velocity is set to 0.2 mm/s and displacements are recorded at both ends of the gauge area with tactile sensors. In principle, uniaxial tension tests can also be used for the identification of the damage parameters. However, when a finite-element model is used to inversely determine the damage parameters, it is advantageous to exploit symmetries. This requires that the fracture behaviour and in particular the crack pattern exhibits symmetries as well. In uniaxial tension tests, the crack path might be influenced by minor asymmetries in the manufacturing process. The advantages of the described notched tensile specimen are that the crack-path is completely perpendicular to the surface and that the crack-paths are highly reproducible in repeated experiments.

### 3.3 Identification strategy

The material parameters ($C$, $\varepsilon_0$, $n$) which describe the isotropic Swift hardening behaviour are directly determined from the flow curve for the pre-necking response. Since the displacement field is inhomogeneous at the onset of plasticity in the notched geometry, the analysis and subsequent parameter identification scheme has to consider this. Thus the damage parameters are obtained by inverse parameter identification. This requires the set-up of an FE-model of the notched geometry and application of a suitable optimization algorithm. Due to the local nature of damage and subsequent fracture a high spatial resolution of the FE-model is needed. A large number of degrees of freedom lead to larger computation times. Therefore it is desirable to reduce the number of experiments which are considered in the identification process. However, relevant physical phenomena should occur in the selected experiments to allow the proper identification of corresponding material parameters. Since there is no explicit dependence on the triaxiality and the stress state in (10), the material parameters $Y_0$, $\beta$, $\kappa$, $S$, which appear in (10) and govern the evolution of damage, are determined with the help of a single notched geometry.
The isotropic hardening parameters ($C$, $\varepsilon_0$, $n$) are kept constant in the optimization procedure. The threshold for the loss of load bearing capacity $D_C$ can be determined a posteriori after the identification of the other damage parameters as it has no effect on the evolution of damage. In the FE-simulation, the stiffness of elements with $D \geq D_C$ is set to zero and their further processing is skipped. The parameter $h$, which weights the influence of negative principal stresses and triaxiality, does not influence the model response for positive triaxialities. Blanking simulations, where an influence of the particular value of $h$ is expected, are performed to analyse the influence. A qualitative study using a simplified analytical approach is performed prior to the full scale parameter optimization. This serves the purpose to generate good starting values and helps to assess which influence a single parameter has on the physical response. In this investigation a homogeneous uniaxial stress state is assumed. Due to the complexity of the Lemaitre damage model it is not straight-forward to see the direct influence of single parameters on a physical response like a force.

*Set-up of FE-simulations of tensile tests with notch*

The commercial software Abaqus Explicit in combination with a VUMAT implementation of the described material model is used for the simulation of the tensile test with the notched

specimen geometry and the blanking process. As the current material model is a local damage model, a mesh-size dependency as observed for the Gurson model in Soyarslan et al. [9] is expected. Therefore, the smallest edge length in the simulations of the tensile test should be similar to the smallest element length in the blanking simulation. As the crack-path of the chosen specimen is completely perpendicular to the surface, all three symmetries are exploited and only one eighth of the total specimen is modelled with eight-node hexahedral elements (C3D8R). Two different spatial discretisations (minimum edge length 0.05 mm to 0.1 mm) are investigated to assess the effect on the corresponding parameter identification.

*Optimization strategy*

As a target function for minimization the least square error

$$e = \sum_{i=1}^{N} \sqrt{\left( F(u_i)_{\exp,i} - F(u_i)_{sim,i} \right)^2} \tag{11}$$

is selected. $F(u_i)$ represents the value of the force recorded in the tensile experiment at the cross-head displacement $u_i$. The indices “exp” and “sim” refer to the response obtained in the experiment and the simulation, respectively. The optimization starts with initial values obtained from preliminary simulations and the analytical assessment mentioned above. The optimization itself is performed with the software LS-OPT from LSTC [10]. The least square error $e$ depends on the material parameters $Y_0$, $S$, $\kappa$ and $\beta$. The optimization finds a suitable set of these parameters, which minimizes the least square error $e$. LS-OPT evaluates 8 different parameter sets per iteration.

### 3.4 Set-up of blanking simulations and experiments

Blanking simulations are performed to study the evolution of the stress state and the corresponding damage evolution. It is shown how the choice of material parameters affects the predicted geometry of the cutting surface. The blanking process is modelled using axis-symmetric elements with a minimum element size of 0.005 to 0.010 mm in the designated shear zone. A penalty contact algorithm is selected. The effect of friction is considered by the Coulomb friction model with a constant assumed coefficient of 0.1. The tools are modelled as discrete rigid bodies. After every three time increments an Arbitrary-Lagrange-Euler (ALE) step will adjust the topology of the mesh in the cutting clearance (area between the tools) to avoid severe mesh distortion. Details of the applied ALE scheme can be found in [11].
For a qualitative comparison of simulations and experiments blanking experiments are performed on a Schuler Servo press with a maximum force of 4000 kN. Punch and matrix have a radius of 0.03 mm. The cutting clearance is 0.1 mm and thus 10% of sheet thickness of the tested DP600. The punch has a diameter of 16 mm. The velocity at the instance of first contact between punch and blank is approximately 16 mm/s. The strain rate is thus expected to have a dimension of 10 1/s. Blanking experiments are conducted on the high-strength low alloyed (HSLA) steel HC300LA (yield point between 300 and 380 MPa, according to manufacturer).

### 3.5 Single-Element under tensile load

As full scale FE-simulations require considerable computing time, it is advantageous to study simplified analytical models to obtain a precise impression of a single material parameter's influence on a relevant physical quantity. It is assumed that the loading is tensile and completely uniaxial. Furthermore the stress state is perfectly homogenous. Apart from the damage parameter, which is varied in the specific evaluation, the other damage evolution parameter have been set to one and the representative values are chosen for the other parameters.

## 4 RESULTS AND DISCUSSION

The presentation of the results and the corresponding discussion starts with the analysis of the model uniaxial tension test. It continues with the qualitative analysis of the influence of the damage parameters on a force-displacement curve. Afterwards the triaxiality in the deformation zone between punch and die is analysed to assess the distribution of low and negative triaxiality in space and time. The presentation of the results ends with a demonstration of the necessity to apply a material model which considers the retardation of damage evolution for compressive stress states.

### 4.1 Qualitative influence of damage parameters

Figure 1 presents a short analysis on the qualitative effect of the parameters $S$, $\kappa$ and $\beta$ on the global force-displacement curve for homogeneous uniaxial tension, according to the simplified model. For simplicity the fourth evolution parameter $Y_0$ has been set to zero, because it can be seen from (10) that it is a threshold for the initiation of damage. The relative force $F/F_{\max}$ and relative displacement $u/u_{\max}$ are shown. Checks with the sophisticated simulations showed qualitatively comparable agreement.

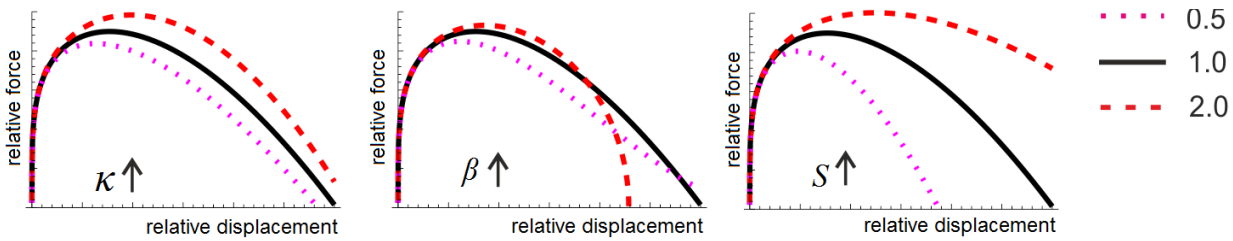


**Figure 1**: Qualitative comparison of damage evolution parameters on the force-displacement-curve of a uniaxial tensile test. In each graph the indicated parameter is changed from 0.5 over 1.0 to 2.0, while all other evolution parameters are set to 1.0. Other parameters are set with characteristic model data.

At first glance, all parameters are apparently independent from the other ones. An increasing $\kappa$ shifts the post-necking regime from bottom left to upper right, while total displacement at zero force is hardly affected. The effect of $\beta$ can be described with the magnitude and duration of curvature in the post-necking region. While increasing $\beta$ means a more sudden drop in load carrying capacity and decreased fracture displacement, values for $\beta$ smaller than one result in a smooth fading out of load carrying capacity to theoretically possible infinity. These observations match with a detailed glance at the evolution term. While $\kappa$ is the exponent of

the term including the driving force for damage $Y$ (see (10)), the parameter has the strongest influence in the early regime, when the accumulated damage is low. $\beta$ on the other hand affects the term (1-$D$) with the accumulated damage and thus determines how strong previous damage accelerates the growth of new damage. Finally an increasing $S$ results in a decreasing slope of the force-displacement curve after necking. Thus the fracture displacement becomes larger. An interesting aspect for further research would be, whether in spite of this first evaluation of the damage evolution parameter, one of these parameters could be omitted because there might be a dependency.

### 4.2 Identified parameters for DP600

Due to these observations an improved initial guess was used for the optimization of the damage parameters, such that a suitable set was obtained after approximately 12 iterations. Table 1 lists the parameter sets found for the damage model for two discretisations.

**Table 1**: Identified set of damage parameters for DP600

| Element size | $Y_0$ | $S$ | $\kappa$ | $\beta$ | $D_C$ |
|---|---|---|---|---|---|
| 0.1 mm | 0 MPa | 59 | 0.44 | 0.32 | 0.21 |
| 0.05 mm | 0 MPa | 60 | 0.5 | 0.37 | 0.22 |

While $Y_0$, $S$ and $D_C$ seem independent from the element-size (based on the current results), $\kappa$ and $\beta$ exhibit a stronger dependency on the mesh size.

### 4.3 Stress state in cutting zone

It is general consensus to assume that the deformation state in the cutting zone is dominated by simple shear stress states and that correspondingly, the triaxiality is ≈ 0 [12, 13]. Two parameters, the relative punch displacement $u_\mathrm{P} = u/t$ and the relative punch displacement at fracture $u_r = u/u_f$ are introduced to describe the kinematics of the cutting process. $t$ is the sheet thickness and $u_f$ the punch displacement at fracture. The punch displacement at fracture determines the state, when complete separation is achieved. For small punch penetrations ($u_\mathrm{P} < 10\%$), the triaxiality is ≈ -1/3 (Figure 2 a)). This triaxiality value is characteristic for uniaxial compression. When $u_\mathrm{P} = 20\%$ the dominating triaxiality is approximately zero (Figure 2 b)), corresponding to the shear state. This state continues until $u_\mathrm{P} = 30\%$, when triaxiality becomes mainly positive which is typical for tensile states (Figure 2 d)). From then the triaxiality rises rapidly to 1 at ultimate fracture (Figure 2e)). Thus a vast range of triaxiality is passed during the deformation in the blanking process. Remarkably, this is a monotonic trend from moderate negative to very high positive triaxiality. Table 2 summarizes the above described information.
Further investigation of Figure 2 reveals that in the pictures (a) ,b), c)) no crack has initiated and thus all material separation is due to shear. On the other hand in (d) ,e)) a crack initiates at both tool edge radii (punch and die). Firstly no interaction is observed and the cracks grow parallel to the travelling punch. Just when the stresses become hydrostatic the cracks change their direction and grow towards each other (not pictured).

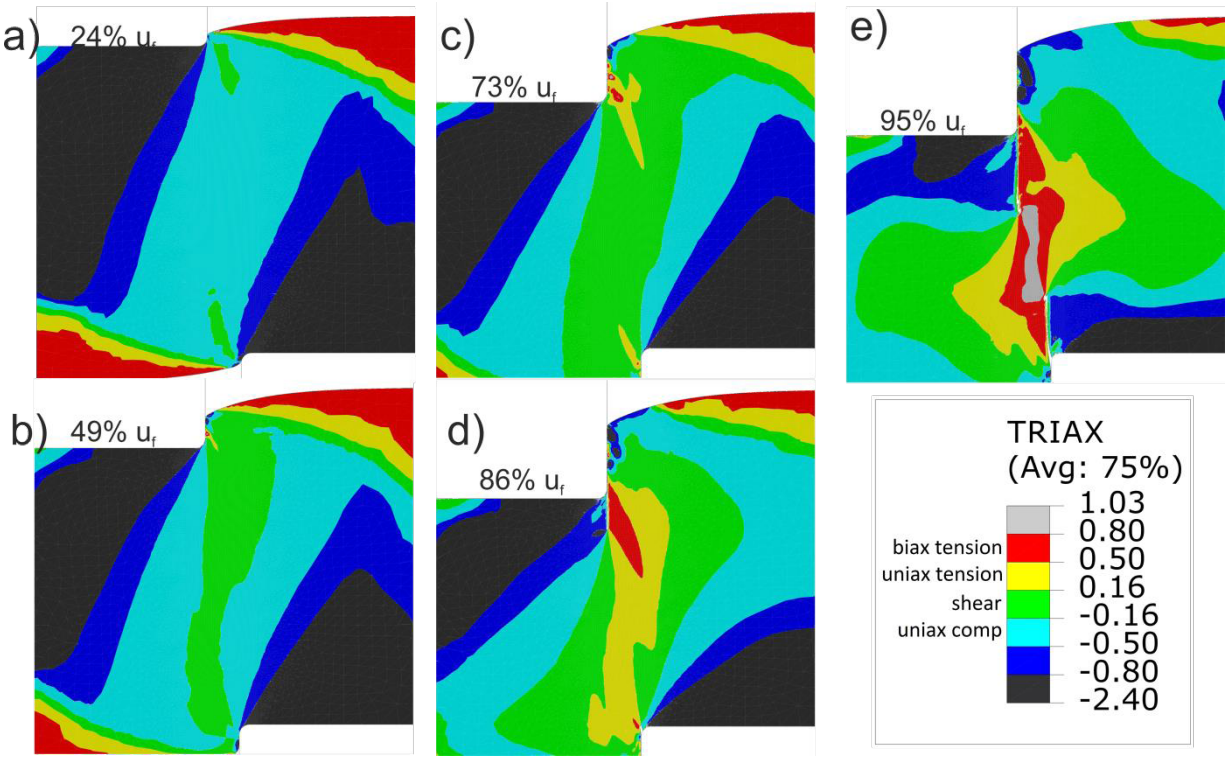


**Figure 2**: Triaxiality in the deformation zone at different punch displacements. $u_f$ is the total displacement until complete separation of the material.

**Table 2**: Summary of triaxiality fractions in the process of blanking. Apart from the mixed stress states the pure uniaxial compression and uniaxial tension have considerable influence on the separation process.

| Relative Punch Penetration $u_P$ | Fraction of failure displacement $u_r$ | Characteristic stress state (triaxiality) | Duration $\Delta u_f$ |
|---|---|---|---|
| 0% - 12% | 0% - 32% | Uniaxial compression | 32% |
| 12% - 18% | 32% - 49% | Mixed | 17% |
| 18% - 27% | 49% - 73% | Shear | 24% |
| 27% - 32% | 73% - 87% | Mixed | 14% |
| 32% - 37 % | 87% - 100 % | Tension | 13% |

### 4.4 Influence of damage modelling on cutting surface

As mentioned before in Section 2 the enhanced model is capable of modelling quasi-unilateral damage growth. While $h = 1$ corresponds to the standard Lemaitre model, $0 \leq h < 1$

matches the observation of Bao et al. [8] and other researches that negative triaxiality stress states have a weakened to almost vanishing influence on damage evolution. With this description in mind it is very interesting to investigate the influence on the cutting surface (Figure 3). For this purpose the evolution of the damage variable *D* during the blanking

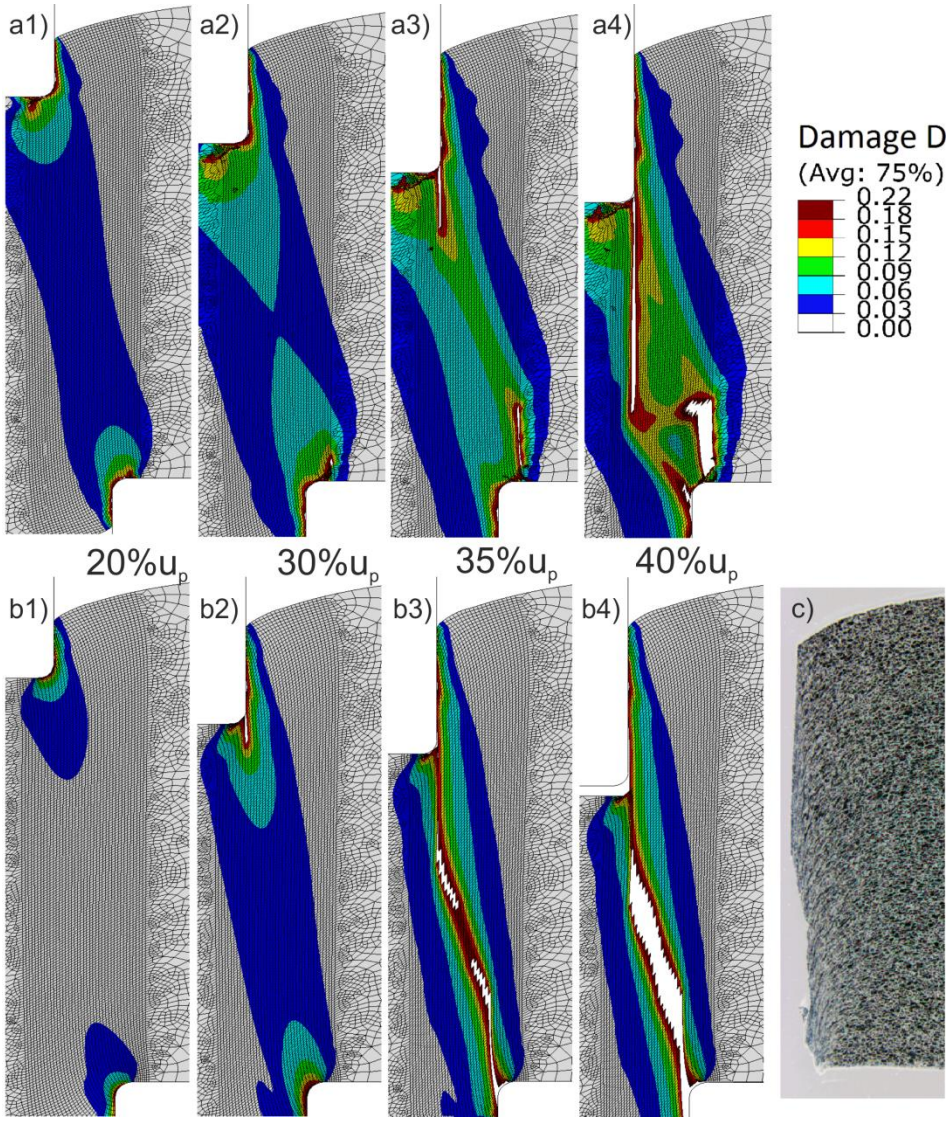


**Figure 3**: Simulated cutting surface of DP600 for different *h*-parameters 1.0 (top, a1) - a4)) and 0.2 (bottom, b1)-b4)). Pictures with the same numeric index are captured at the same displacement. On the right(c): Exemplary micro-graph of cutting surface of micro-alloyed steel HC300LA for qualitative comparison.

process is analysed for different values of the parameter *h*. The top row (a1) – a4)) corresponds to the original model (*h* = 1), while the lower row (b1) – b4)) shows results for *h* = 0.2. Note that Figure 3 contains complementary information to Figure 2.

The pictures indexed with 1 (Figure 3 a1), Figure 3 b1)) correspond to a relative punch displacement $u_p = 20\%$ (cf. Figure 2b)). Thus the accumulated damage in the cutting zone at this state results only from stress states with a negative triaxiality. The pictures indexed with 2

(a2), b2)) correspond to a relative punch displacement $u_P = 30\%$ (Figure 2c)). Due to the change in stress state mainly in the cutting zone damage has also accumulated under the influence of a shear stress state. While in the simulation, which considers the retardation of damage evolution ($h$ = 0.2), a crack initiates at the outer punch (Figure 3 b2)) the original Lemaitre model does not predict such a crack (Figure 3 a2)). Instead the crack initiation is predicted at the die. Remarkably it nucleates far away from the die radius, which seems unphysical. A glance at Figure 2c reveals, that this region exhibits a negative triaxiality with a large magnitude. As the original Lemaitre model does not distinguish between compression and tension, it predicts a high driving force for damage evolution. The analysis of relative punch displacements $u_P > 35\%$ (Figure. 3 a3)), Figure 3 b3)) reveals that the two model variants predict separation of the sheet for different punch displacements. For even larger punch displacements $u_P > 40\%$ (Figure 3 a4)), Figure 3 b4)) even larger qualitative differences are observed. Not just the necessary punch displacement, but the fracture surfaces differ completely. While for the modified model ($h$ = 0.2) the two initiated cracks grow towards each other in an acute angle, for the original model ($h$ = 1) the cracks coalesce in a right angle. For qualitative comparison Figure 3c) shows exemplarily the experimental cut surface of a micro-alloyed steel (HC300LA) to emphasize the necessity for the application of the modified model.

## 5 CONCLUSION

An enhanced Lemaitre damage model which considers the effect of compressive stresses on damage evolution has been investigated in a twofold manner. Initially an efficient strategy for parameter identification was described. This was accompanied by an extended study of the influence of single parameters on failure prediction. Further investigations should reveal, whether one parameter can be replaced due to dependencies.

The second focus was on the investigation of the deformation zone during blanking. The presented work has revealed that for more than a quarter of the total punch stroke during blanking uniaxial compression is the pre-dominant stress state during the deformation process. Other stress states, which occur in the cutting zone are shear, uniaxial tension and mixed states. This emphasizes that for a physically based modelling, the effect of shear and compression stress states on damage and fracture have to be considered. Furthermore it has been found that in the vicinity of the edge radii of the tools the magnitude of the stress triaxiality is high. On the inner side of the edge, which lies in the horizontal gap between punch and die the triaxiality has high positive values which decrease and evolve to high negative triaxiality on the outer side. Thus a material model, which can distinguish the effect of negative and positive triaxialities on damage, is crucial to prevent unphysical crack paths. In further research, a more detailed comparison between blanking experiments and simulations involving an extended material characterization will be performed for DP600.

## 6 ACKNOWLEDGEMENT

FG appreciates financial support from the German Research Foundation (DFG) in the project DFG 1 Te 508/37-1. FS acknowledges financial support of IGF project 16585 N coordinated by FOSTA - Research Association for Steel Application - was supported by the AiF under the program for the promotion of industrial research by the Federal Ministry of Economics and

Technology based on a decision by the German Bundestag. Both projects are embedded in the Research-Cluster PAK 678/0 “Dry Shear Cutting of Metal Laminated Composite Material” supported by DFG and Arbeitsgemeinschaft industrieller Forschungsvereinigungen “Otto von Guericke” e.V. (AiF).

## REFERENCES

[1] Goijaerts, A.M., Govaert, L.E., Baaijens, F.P.T. Evaluation of ductile fracture models for different metals in blanking. *J. Mat. Proc. Tech.* Vol. 11, pp. 312-323 (2001)

[2] Hambli, R., Potiron, A. Finite element modelling of sheet-metal blanking operations with experimental verification. *J. Mat. Proc. Tech.* Vol. 102, pp. 257-265 (2000)

[3] Hambli, R. Comparison between Lemaitre and Gurson damage models in crack growth simulation during blanking process. *Int. J Mech. Sci.* Vol. 43, pp. 2769-2790 (2001)

[4] Dalloz, A, Besson, J., Gourgues-Lorenzon, A.-F., Sturel, T., Pineau, A. Dffect of shear cutting on ductility of a dual phase steel. *Engrg. Frac. Mech.* Vol. 76, pp. 1411-1424 (2009)

[5] Lemaitre, J. and Desmorat, R. *Engineering Damage Mechanics*. Springer, (2005).

[6] Soyarslan, C., Tekkaya, A. E. A damage coupled orthotropic finite plasticity model for sheet metal forming: CDM approach, *Comp. Mat. Sci.* Vol. 48(1), pp. 150-165 (2010).

[7] Lemaitre, J. Evaluation of dissipation and damage in metals. Proceedings of I.C.M. 1. Kyoto, Japan (1971).

[8] Bao, Y., Wierzbicki, T. On fracture locus in the equivalent strain and stress triaxiality space. *Int. J. Mech. Sci.* Vol. 46(1), pp. 81-98 (2004)

[9] Soyarslan, C., Malekipour Gharbi, M. Tekkaya, A. E. A combined experimental-numerical investigation of ductile fracture in bending of a class of ferritic-martensitic steel, *Int. J. Sol. Struct.*, Vol. 49 (13), pp. 1608-1626 (2012)

[10] LS-OPT Version 5.0, April 2013, Livermore Software Technology Corporation (LSTC)

[11] Abaqus 6.11 Analysis User’s Manual, Vol. 5, Dassault Systèmes Simulia Corp.

[12] Martins, P.A.F., Atkins, A.G. Revisiting the empirical relation for the maximum shearing force using plasticity and ductile fracture mechanics. J. Mat. Proc. Tech. Vol. 213, pp. 1516-1522 (2013)

[13] Klingenberg W., Singh, U.P. Comparison of two analytical models of blanking and proposal of a new model. Int. J. Mach. & Manuf. Vol. 45, pp. 519-527 (2005)